

## Growth of Silicon-Germanium Alloy Layers

C.K. Maiti, L.K. Bera, S. Maikap, S.K. Ray and N.B. Chakrabarti  
*Indian Institute of Technology, Kharagpur-721 302*

and

R. Kesavan and V. Kumar  
*Solidstate Physics Laboratory, Delhi-110 054*

### ABSTRACT

Heteroepitaxy techniques for the growth of group IV binary alloys, in particular,  $SiGe$ ,  $SiC$ ,  $GeC$  and  $SiSn$  films are reviewed. Deposition of heteroepitaxial films using various reactors like molecular beam epitaxy, gas source molecular beam epitaxy, and different chemical vapour deposition techniques are compared. Issues related to heteroepitaxial film deposition, such as critical layer thickness are examined. Growth of strained silicon on relaxed  $SiGe$  buffer layers, poly- $SiGe$  film and hydrogenated amorphous  $SiGe$  ( $a^2SiGe:H$ ) film is also reviewed.

### 1. INTRODUCTION

The advances in crystal growth technologies, such as molecular beam epitaxy (MBE), gas source molecular beam epitaxy (GSMBE), organometallic vapour phase epitaxy (OMVPE), and chemical vapour deposition (CVD) have enabled ultra thin epitaxial semiconductor layers to be routinely grown with monolayer precision in thickness and composition control to about one atomic per cent. In the past, main focus was on homoepitaxial films and closely lattice-matched combination of materials such as  $Al_xGa_{1-x}As/GaAs$  and  $In_{0.53}Ga_{0.47}P/InP$ . The possibilities for lattice-matched heteroepitaxial systems are relatively limited as shown in Fig. 1. In the last decade, focus was placed on lattice mismatched combination of materials as these material systems also offer unique new prospects, such as the use of strain to modify electronic and optical properties. Recently, alloys of group IV elements, including carbon, silicon, germanium and tin have been actively pursued for use in heterojunction devices compatible with conventional silicon processing technology. Major

advancements have been made in binary  $SiGe/Si$  alloys where the built-in strain and the composition of a pseudomorphic  $Si_{1-x}Ge_x$  layer on silicon substrate affect the band structure, energy gap as well as the band offset significantly. High performance devices and circuits based on  $Si/Si_{1-x}Ge_x$  heterostructures have been demonstrated. There is now considerable literature on various aspects of  $Si_{1-x}Ge_x$  epitaxial growth and devices<sup>1-4</sup>.

Strain-induced modification of  $Si/SiGe$  films have a significant impact on the band structure and carrier transport. When a thin film with a larger lattice constant (e.g.  $Si_{1-x}Ge_x$ ) is grown on a smaller lattice constant substrate (e.g. silicon), the film maintains in-plane lattice constant of the substrate and is under a biaxially compressive strain. Figure 2 shows the band offset between a strained  $Si_{0.7}Ge_{0.3}$  film grown on silicon. This is known as the *type-I* band alignment where the entire band offset occurs in valence band [Fig. 2(a)] while band offset in conduction band is very small. This type of structure is favourable for hole confinement

Table 1. Summary of deposition systems

	MBE	Gas source MBE	UHV-CVD	LRPCVD/ RTCVD	VLPCVD	Atmospheric CVD
Base pressure (Torr)	$10^{-10}$	$10^{-10}$	$10^{-10}$	$10^{-3}$ to $10^{-7}$	$10^{-7}$ to $10^{-8}$	
{In situ} cleaning	Yes	Yes	No	Yes	Yes	Yes
Source		$SiH_4, GeH_4$	$SiH_4, GeH_4$	$SiH_4, GeH_4$	$SiH_4, GeH_4$	$SiH_4, GeH_4$
Gas		$SiH_4$	$SiH_4$	$SiH_4$	$SiH_4$	$SiH_4$
Dopant gas	$B_2H_6, AsH_3, PH_3$	$B_2H_6, AsH_3, PH_3$	$B_2H_6, AsH_3, PH_3$	$B_2H_6$	$B_2H_6, AsH_3, PH_3$	$B_2H_6, AsH_3, PH_3$
Deposition temperature ( $^{\circ}C$ )	$< 550$	550-625	550	625-850	625-850	$< 350$
Deposition pressure (Torr)	$10^{-8}$	$10^{-4}$	$10^{-3}$	0.2	$10^{-3}$	
$Si_{1-x}Ge_x$ (x=per cent)	0-100,		0-100	$< 40$	$< 15$	Atm
Film deposition	$SiC, SiGe, SiGe$ $GeC, GeSn$					
{In situ} doping	Difficult	Yes	Yes	Yes	Yes	
Selective epitaxy	No	Yes	Yes	Yes	Yes	Yes

and has been exploited in several novel heterostructure<sup>5</sup> devices, viz., buried channel *p*-MOSFETs, *p*-MODFETs and HBTs.

Similarly, a smaller lattice constant silicon epilayer will be under biaxial tension when grown on a

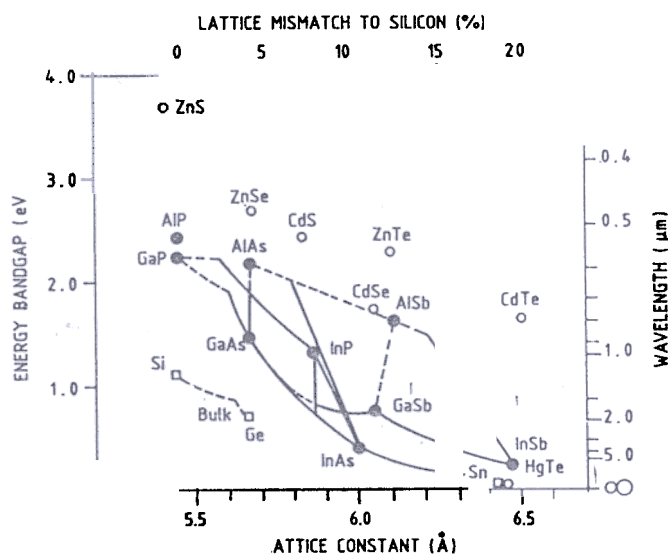


Figure 1 Plot of semiconductor lattice constant,  $a_0$ , vs minimum bandgap,  $E_g$ , for column IV, II-VI, and III-V semiconductors. Lines indicate bandgap for alloy of semiconductors at end points. Solid line denotes a resulting direct minimum bandgap. Dashed line an indirect bandgap. Also shown are photon energies equivalent to the minimum bandgap and percentage lattice mismatch to silicon's 5.42 Å lattice constant.

larger lattice constant relaxed  $Si_{1-x}Ge_x$  substrate. Figure 2(b) shows the band offset for a strained silicon epilayer grown on a relaxed  $Si_{0.70}Ge_{0.30}$ . In this case, *type-II* band offset occurs and the structure has several advantages over the more common *type-I* band alignment, as a large band offset is obtained in both the conduction and valence bands, relative to the relaxed  $Si_{1-x}Ge_x$  layer<sup>6</sup>. This allows both electron and hole confinements in strained silicon layer making it useful for both *n*- and *p*-type devices for strained *Si/SiGe*-based CMOS technology. Since strained silicon provides both larger conduction and valence band offsets and does not suffer from alloy scattering<sup>7</sup> (hence mobility degradation), a significant improvement in carrier mobility can be achieved. Strained silicon is more difficult to grow compared to strained  $Si_{1-x}Ge_x$ , since bulk  $Si_{1-x}Ge_x$  substrate is currently not available and until recently, growth of relaxed  $Si_{1-x}Ge_x$  without forming large concentration of defects due to dislocation was difficult. However, the ability to achieve both *n*-MOS and *p*-MOS devices using strained silicon provides a promising alternative for next-generation high performance *SiGe*-CMOS technology<sup>8,9</sup>.

In this paper the growth of group IV binary alloy films has been reviewed. The deposition of heteroepitaxial films using various reactors has been critically examined. As the reactor configurations differ substantially, the advantages and disadvantages

of each system are compared. The deposition and characterisation of binary  $Si_{1-x}Ge_x$ ,  $Si_{1-y}C_y$ ,  $Ge_{1-y}C_y$ , and alloy layers containing tin are discussed. Growth of strained silicon on relaxed  $SiGe$  buffer layers, poly- $SiGe$  film and hydrogenated amorphous  $SiGe$  (a- $SiGe:H$ ) film is also considered.

## 2. GROWTH OF BINARY ALLOY LAYER FILMS

$SiGe$  alloys have attracted considerable attention during the last decade, and it is now recognised that the  $Si/Si_{1-x}Ge_x$  material system is the most practical route to heterojunction devices on silicon substrates. The present review emphasises  $Si/SiGe$  technology that can be integrated into silicon processes. The growth of other binary alloys, such as silicon-carbon, silicon-tin, and germanium-carbon for each of these material system has its own merit. In applications of strained silicon layers, it is important to grow thick relaxed  $SiGe$  layers as buffer. Poly- $Si_{1-x}Ge_x$  and hydrogenated amorphous  $SiGe$  (a- $SiGe:H$ ) films have applications as gate electrodes and interconnects in integrated circuits, thin film transistors (TFTs) for flat panel displays and high efficiency multijunction solar cells, respectively.

Most of the early work on binary  $Si_{1-x}Ge_x$  alloy films was carried out using MBE whereas growth using CVD systems started much later. A comparison of different deposition systems is given in Table 1.

### 2.1 Growth of $Si_{1-x}Ge_x$ Films

In case of strained layer epitaxy, lattice mismatched strained layers can be grown without misfit dislocations if the thickness is kept below the critical thickness. The stability of strained layers was first studied by Frank and Van der Merwe<sup>12</sup>.

The term critical thickness was initially defined to denote the transition from a strained to relaxed layer. Using a continuum model, authors calculated the critical layer thickness,  $h_c$ , below which the strained layer is expected to be in the thermodynamically stable state. Above  $h_c$ , it is energetically favourable to relieve the strain *via* dislocations. Since then, there have been a number<sup>6,13-16</sup> of reports on calculations of  $h_c$  differing from each other in the assumed energy stored in a dislocation. Van der Merwe<sup>17,18</sup> was the first to calculate the critical thickness as a function of increased lattice mismatch by minimising

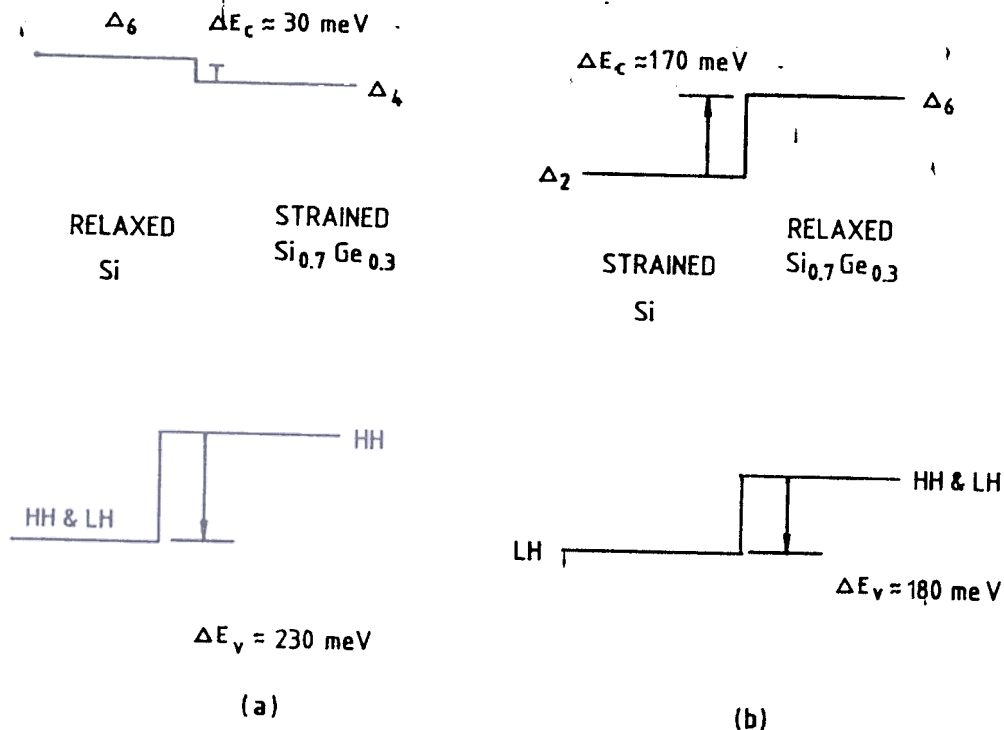


Figure 2. Band alignments between silicon and  $Si_{0.70}Ge_{0.30}$  on two substrates: (a) silicon and (b)  $Si_{0.70}Ge_{0.30}$

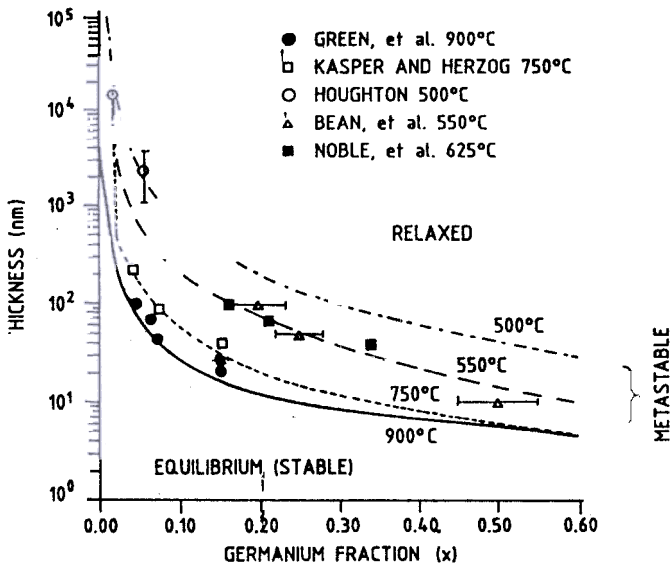


Figure 3. Critical thickness of  $Si_{1-x}Ge_x$  layers as a function of germanium mole fraction. Lines show theoretical kinetic model for various growth temperature.

the sum of the interfacial and strain energy. However, recently published literature has embraced the mechanical equilibrium theory of Matthews and Blakeslee<sup>13,19</sup> as defining the transition from the stable to metastable regimes. Figure 3 shows three regimes in the plot of  $Si_{1-x}Ge_x$  layer thickness on silicon versus germanium concentration ( $x$ ). The germanium concentration is directly related to the lattice mismatch according to Vegard's law. Bean<sup>20</sup>, *et al.* deposited strained layers by MBE at 550 °C with a thickness of an order of magnitude or more above the Matthews-Blakeslee curve as shown by the solid data points (Fig. 3). The measured critical thickness depends on growth temperature and growth rate. This was proved experimentally that  $h_c$  increases with decreasing substrate temperature<sup>16,21</sup>. The dotted line joining these data points demarcates the metastable and dislocation regimes. Between the solid mechanical equilibrium line and the dotted MBE data points, layers are labeled metastable. Layers in the metastable regime are strained even though the layers are above the Matthews-Blakeslee critical thickness. However, metastable layers relax with subsequent annealing. Above the dotted line, Bean,<sup>20</sup> *et al.* found that strained  $Si_{1-x}Ge_x$  layers were impossible to deposit. People and Bean<sup>16</sup> sought to reconcile these differences by including the kinetics of relaxation in their calculation and the critical thickness prediction

fits their experimental data. Many other researchers have contributed for critical thickness theories based on energy, mechanical equilibrium, and kinetics of dislocations<sup>22-24</sup>.

The first trial of  $Si_{1-x}Ge_x$  growth on silicon was attempted in 1977 by Kasper<sup>25</sup>, *et al.* at 750 °C using MBE. As the temperature was high, three-dimensional growth took place and islanding was observed. The first commensurate growth of  $Si_{1-x}Ge_x$  layer on silicon was reported by Bean<sup>20</sup>, *et al.*, who used a low temperature (550 °C) growth technique. At this low temperature, it was found that the critical thickness of the epilayer was several times higher than the value that can be obtained from the mechanical equilibrium theory<sup>13</sup>. The key feature of this low temperature growth is that two-dimensional growth of strained  $Si_{1-x}Ge_x$  containing a high concentration of germanium is possible. For example, for a pseudomorphic growth of  $Si_{0.5}Ge_{0.5}$  on silicon, the growth temperature must be lower than 550 °C. Bean<sup>20,26</sup>, *et al.* found that the maximum germanium incorporation before the occurrence of non-planar growth depends on the deposition temperature, as shown in Fig. 4. At 750 °C, the maximum germanium mole fraction is 10 per cent,

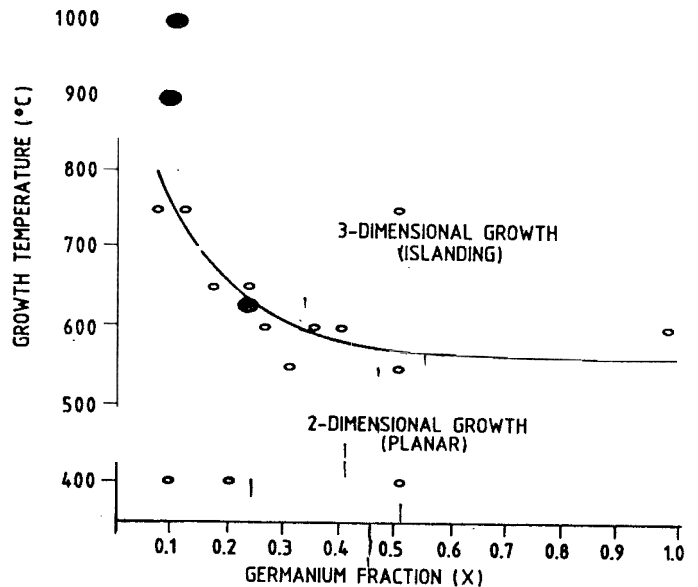


Figure 4. Plot of growth regimes vs growth temperature and mole fraction ( $x$ ) for  $Si_{1-x}Ge_x$  grown on silicon substrates. The solid line and the open circles refer to MBE, while the solid circles refer to LRP samples which exhibit planar growth.

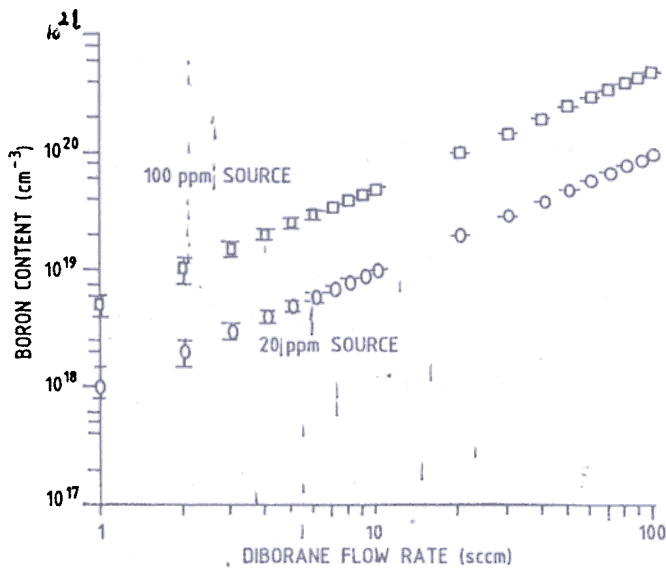


Figure 5. Dopant accuracy for two dopant source concentrations. Limitations are flow controller absolute accuracy and offset, as well as temperature-induced fluctuations.

whereas at 550 °C, 100 per cent germanium mole fraction is possible. It is speculated that higher deposition temperatures resulted in surface mobility, high enough to cause surface tension problems and islanded growth. Deposition rates of up to 600 nm/min for silicon are possible. However, typical  $Si_{1-x}Ge_x$  deposition rates are in the 30 nm/min range for greater profile control<sup>26</sup>. Also, extremely abrupt compositional profile control is possible by the use of mechanical shutters. At 630 °C, the  $Si_{1-x}Ge_x$  growth rate decreases with increasing germane ( $GeH_4$ ).

Ultra high vacuum chemical vapour deposition (UHVCVD) system developed by Meyerson<sup>27</sup>, *et al.*, uses base pressure of  $10^{-9}$  Torr, growth pressure of  $10^{-6}$  Torr, and a growth temperature as low as 550 °C. This system, however, has few limitations. As the source gas flow is increased (at constant temperature) to increase the germanium concentration during a  $Si_{1-x}Ge_x$  layer growth, the growth rate increases.

The deposition pressure is about 1-2 mTorr with deposition rates around 1-2 nm/min. Because of the low deposition pressure, gas depletion does not occur like in standard low pressure chemical vapour deposition (LPCVD) polysilicon reactor at 0.4 Torr. *In situ* doping of both types is possible!

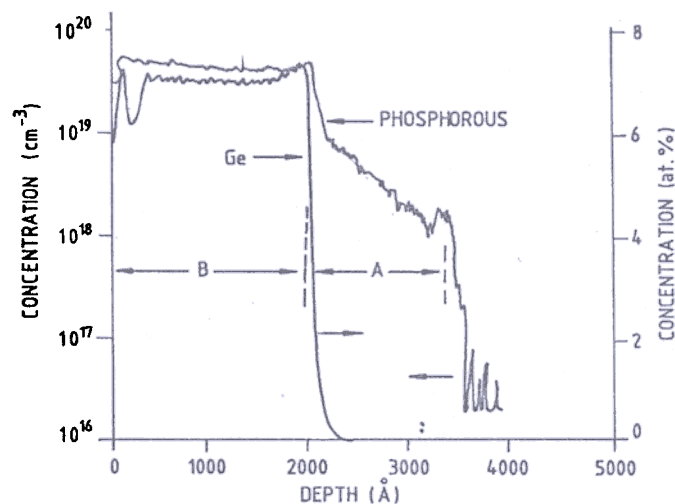


Figure 6. Film phosphorous content, by SIMS, as influenced by the addition of germane during UHVCVD film growth. Silane and phosphine flows were constant throughout growth (regions A and B), while germane was added at a constant flow in region B. Spreading resistance showed the phosphorous to be fully activated.

and boron dopant content in the film is linear as shown in Fig 5. The addition of  $PH_3$  to silane ( $SiH_4$ ) produces *n*-type doping. Although dopant control is similar to that of boron, the dynamic range over which *P* content remains stable is far more limited as shown in Fig. 6 and allows the incorporation of up to  $\approx 1 \times 10^{20} \text{ cm}^{-3}$  (Note the discontinuous jump in, and subsequent stability of, phosphorous incorporation in the presence of germanium). Apparently no problems with islanded growth at high germanium concentrations appear, because the deposition temperature is below 550 °C. The addition of  $GeH_4$  enhances the growth rate of  $Si_{1-x}Ge_x$  over silicon homoepitaxy<sup>28</sup> at 550 °C. The catalytic effect of  $GeH_4$  in removing hydrogen from the surface is cited as the reason for the increased  $Si_{1-x}Ge_x$  growth rate. Germanium incorporation in alloy layers is roughly linear in source germanium content, while the behaviour of growth rate is somewhat more complex, as shown in Fig. 7. Although blanket depositions are trivial, problems appear with patterned oxide depositions because the *HF*-dip cleaning technique is hydrophilic on oxide regions. Polysilicon layers on top of the oxide may eliminate this problem at the expense of greater process complexity. This problem may ultimately limit the manufacturability of the UHVCVD

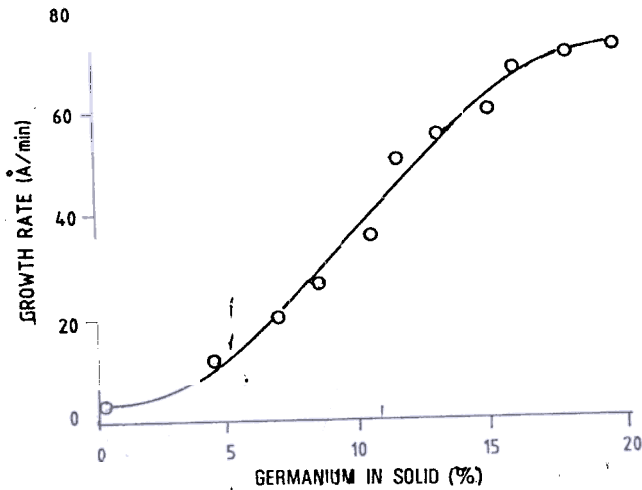


Figure 7. Film growth rate (solid line) during  $SiGe$  UHVCVD as a function of film germanium content. A  $25 \times$  increase in growth rate occurs for the addition of 20 per cent germanium to the solid film.

technique. Selective silicon epitaxy was examined at Tohoku University<sup>29</sup> and selective  $Si_{1-x}Ge_x$  deposition was studied by Greve and Racanelli<sup>30,31</sup>, who observed that  $GeH_4$  enhanced the nucleation time of polycrystalline material on oxide regions of patterned wafers.

Using rapid thermal chemical vapour deposition (RTCVD) growth technique, at a base pressure of  $10^{-7}$  Torr, which is much lower than that used in limited reaction processing (LRP),  $SiGe$  films have been grown<sup>32,33</sup> at 900 °C.  $Si_{1-x}Ge_x$  layers need to be deposited at lower temperatures to avoid relaxation and the three-dimensional growth problems. So the deposition temperature was reduced to 625 °C for  $Si_{1-x}Ge_x$  and increased to 850 °C for silicon cap layers. Fortunately, the  $Si_{1-x}Ge_x$  growth rate increases<sup>34-36</sup> with the addition of  $GeH_4$ . The  $Si_{1-x}Ge_x$  growth rate enhancement with increasing  $GeH_4$  is similar to the UHVCVD result. The maximum incorporation before three-dimensional growth by MBE does not seem to apply to limited reaction processing chemical vapour deposition/rapid thermal chemical vapour deposition (LRPCVD/RTCVD). Layers having up to 45 per cent germanium were deposited<sup>35</sup> at 630 °C. One of the major problems with reducing the temperature is the increased oxygen incorporation in the  $Si_{1-x}Ge_x$  layers. The contamination source was traced to high oxygen content present in  $SiH_2Cl_2$ .  $SiH_4$  does not have the

same problem because the gas with much higher purity is available<sup>32</sup>. The oxygen incorporation problem diminishes with the use of a load-lock and a point-of-use filtration of  $SiH_2Cl_2$ .

Atmospheric pressure chemical vapour deposition (APCVD) has been used to grow good quality epitaxial silicon and  $SiGe$  films<sup>37</sup>. This technique offers temperature flexibility over a wide range, excellent temperature uniformity in the commercial process, and a simple conventional flowthrough design which uses no vacuum pumps. Ultra clean APCVD process has been used to grow films at low temperatures, 550-850 °C, by rigorously minimising oxygen and moisture in the growth environment using load-lock, point-of-use gas purification and ultra clean gas handling<sup>37</sup>.  $Si_{1-x}Ge_x$  layers were deposited over the temperature range from 600-900 °C. At 625 °C, the deposition rate of  $Si_{1-x}Ge_x$  alloy was found to increase with  $GeH_4$  partial pressure; the amount of germanium in the alloy increased rapidly at low  $GeH_4$  partial pressures and appears to approach saturation at higher  $GeH_4$  partial pressures.

The deposition rate depends slightly on the  $SiH_2Cl_2$  partial pressure, with a slight decrease in deposition rate with increasing  $SiH_2Cl_2$  partial pressure at higher  $GeH_4$  partial pressures. The deposition kinetics appear similar to the LRP/RTCVD system since  $SiH_2Cl_2$  and  $GeH_4$  are used. When the deposition rate of the silicon component over the temperature range from 600-900 °C was normalised by the germanium content in the alloy, an Arrhenius-type behaviour was observed with an apparent activation energy of about 1.9-2.0 eV suggesting that the deposition process for silicon is limited by reaction kinetics, rather than by mass transport. The germanium component of the deposition rate behaves quite differently as shown in Fig. 8. In low temperature range (600-650 °C), the deposition rate displays an Arrhenius-type behaviour with an apparent activation energy of 0.7 eV, much lower than that of the silicon component. At higher temperatures, the deposition rate of the germanium component depends only slightly on temperature. Remote plasma-enhanced chemical vapour deposition (RPCVD) has also been used for silicon and  $Si_{1-x}Ge_x$  epitaxy<sup>38</sup>.

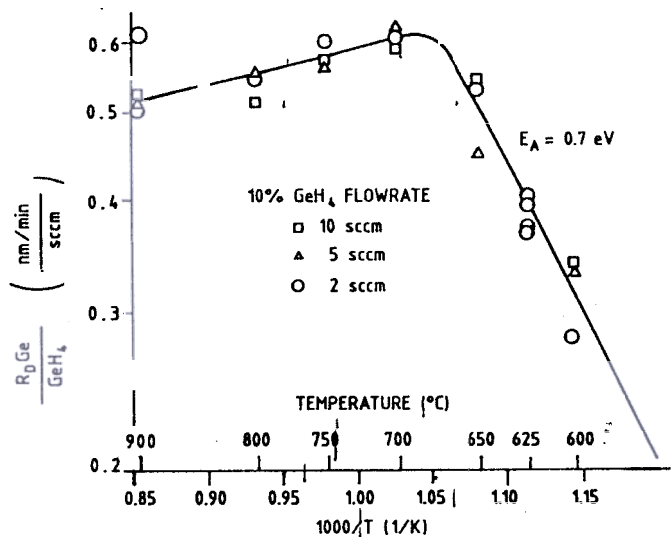


Figure 8. Germanium component of deposition rate normalised by  $GeH_4$  flow.

## 2.2 Growth of $Si_{1-y}C_y$ Films

The growth of  $Si_{1-y}C_y$  epitaxial films on silicon (100) presents a formidable challenge as: (i) the lattice mismatch of carbon is  $-52$  per cent, (ii) carbon has a low solubility in silicon below  $10^{-6}$  at 1400 K, (iii) carbon contamination of silicon surface during epitaxy disrupts the process, and (iv)  $SiC_2$  exists as a stable phase out of several polytypes. The typical conditions for the growth of good quality  $Si_{1-y}C_y$  epitaxial films on silicon by MBE are: (i) growth temperature should be low (typically between  $450$ - $550$  °C), and (ii) an extremely pure elemental C-beam.

Posthill<sup>39</sup>, *et al.* studied the feasibility of deposition of dilute  $Si_{1-y}C_y$  epitaxial films on silicon (100) using RPCVD. Carbon incorporation up to 3 atomic per cent was achieved at a growth temperature of  $725$  °C. The layers were characterised by X-ray diffraction and transmission electron microscopy (TEM). No evidence of the formation of  $SiC_2$  was found.

Extensive work by IBM researchers on the growth of  $Si_{1-y}C_y$  alloys on silicon has been carried out using MBE. Iyer<sup>40,41</sup>, *et al.* and Eberl<sup>42</sup>, *et al.* synthesised pseudomorphic  $Si_{1-y}C_y$  alloys on silicon (100) using solid-source MBE. The layers were characterised by X-ray diffraction, secondary ion mass spectroscopy (SIMS), TEM and Raman

spectroscopy. The researchers demonstrated that good quality layers with a few atomic per cent of carbon ( $y \leq 0.05$ ) can be grown by MBE if a low growth temperature ( $500$ - $600$  °C), and a growth rate of  $0.2$  nms<sup>-1</sup> are used. Amorphous growth occurs for lower substrate temperatures or higher carbon concentration. The thermal stability of  $Si_{1-y}C_y/Si$  strained-layer superlattices was studied by Goorsky<sup>43</sup>, *et al.* The superlattices were grown by MBE as described above, with three concentrations of carbon:  $0.003$ ,  $0.008$  and  $0.013$ . The superlattices were stable on annealing for 2 hr at  $800$  °C. Between  $800$  °C and  $900$  °C, strain relaxation occurred by interdiffusion of carbon and silicon at the interfaces. At  $1000$  °C and above, precipitation of  $SiC_2$  was observed. An X-ray diffraction rocking curve for a ten-period  $Si_{1-y}C_y$  superlattice, taken at glancing angle of incidence<sup>41</sup>, is shown in Fig. 9. Each period of the superlattice consisted of a  $320$  Å silicon layer and a  $110$  Å  $C_{0.005}Si_{0.995}$  layer. The alloy peaks were quite sharp. TEM studies showed no evidence of dislocations or other defects. For 5 per cent carbon concentration, the layers grown at  $450$  °C were amorphous. At higher temperatures, precipitates of  $SiC$  were formed.

One possible application of  $Si_{1-y}C_y$  alloy is the fabrication of symmetrically-strained  $SiC/SiGe$

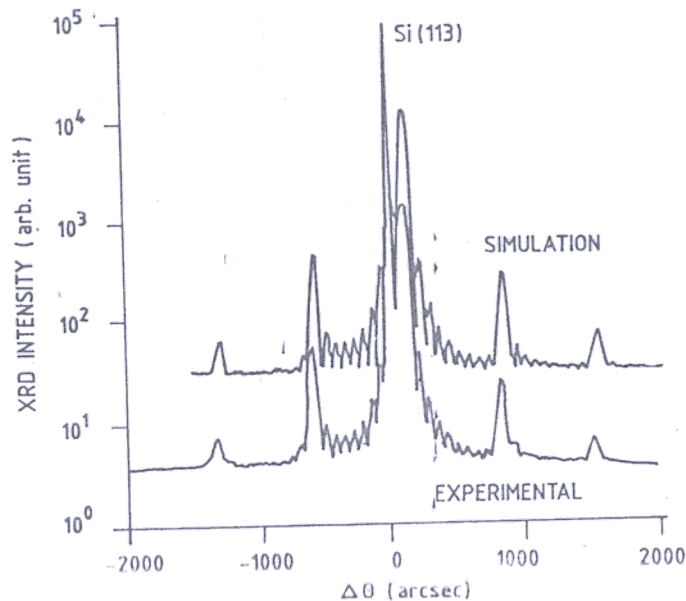


Figure 9. X-ray diffraction rocking curve for an  $Si/Si_{1-y}C_y$  superlattice. The carbon content in the  $Si_{1-y}C_y$  film is  $0.005$ .

superlattices on a silicon substrate. Eberl,<sup>44</sup> *et al.* reported fabrication of  $C_{0.01}Si_{0.99}/Ge_{0.1}Si_{0.99}$  superlattices on silicon. The strain in the superlattices alternates between tensile and compressive in the individual  $Si_{1-y}C_y$  and  $Si_{1-z}Ge_z$  alloy layers, respectively. The individual layer thickness were 10 nm and 13.5 nm, respectively. X-ray rocking curves were measured and average strain in the superlattice was estimated. The strain was considerably less than that expected in a superlattice in which  $C_{0.01}Si_{0.99}$  layer is replaced by an silicon layer. It is clear from these results that perfect symmetrically-strained superlattices can be fabricated by adjusting the relative germanium and carbon content and/or by changing the thickness of the individual layers.

Faschinger<sup>45</sup>, *et al.* reported the electrical properties of undoped and antimony-doped  $Si_{1-y}C_y$  alloys on high resistivity (1000  $\Omega$ -cm) silicon grown by MBE at 500 °C. The layers could be doped with antimony at low growth temperatures (at 350 °C). However, a significant antimony segregation takes place on the surface and leads to doping of the subsequently deposited layers. Modulation-doped  $Si/Si_{1-y}C_y/Si$  structures with the modulation doping in the silicon layer (to avoid unintentional doping of  $Si_{1-y}C_y$  channel and silicon spacer layer) exhibited enhanced electron mobilities with peak values of about 10,000  $cm^2/V.s$  at 100 K, indicating that  $Si_{1-y}C_y$  is strained on silicon and forms an electron channel.

Growth of dilute  $SiC$  epitaxial layers on silicon using RTCVD have been reported<sup>46,47</sup>. Ray,<sup>47</sup> *et al.* reported the growth of polycrystalline and epitaxial layers of metastable  $Si_{1-x}C_x$  alloys using silane and propane at different temperatures with varying amount of carbon ( $x = 0.01, 0.02$  and  $0.05$ ) using RTCVD. Stoichiometric  $SiC_2$  layers were also grown for comparison by increasing propane to silane flow ratio. Following usual cleaning schedules, *p*-type Silicon < 100 > wafers were pretreated with *HF* (2:1) diluted in *DI* water vapour just before loading into the chamber. They have also reported solid phase epitaxy (SPE) growth of  $Si_{1-x}C_x$ . Epitaxial regrowth by rapid thermal annealing of  $C^+$ -implanted silicon and  $SiGe$  layers was used in the study for the formation of metastable phases. *CO* was used as the source gas for *C*-implantation. Ion state was chosen to incorporate 1, 2 and 5 per cent

carbon into silicon with two different energies. All the samples were rapid thermally annealed in nitrogen (1.2 l/min) at 1046 °C for 30 s.

Fourier transform infrared (FTIR) spectroscopic measurements were carried out on all RTCVD and SPE grown layers to study the nature of carbon incorporation. The absorption peaks due to the localised vibrational mode (LVM) of substitutional carbon in silicon at 16.7  $\mu m$  (wave number 607.5  $cm^{-1}$ ) and the strong phonon absorption mode in  $SiC_2$  at 12.6  $\mu m$  (wave number 794  $cm^{-1}$ ) were monitored. Strane<sup>48</sup>, *et al.* reported the synthesis and detailed structural characteristics of  $Si_{1-y}C_y$  strained layers on silicon by SPE. Carbon was introduced into pre-amorphised silicon by multiple energy implantation to form uniform carbon concentration. Pre-amorphisation was done using 60, 30 and 10 keV silicon ions with doses of  $3 \times 10^{15}$ ,  $6 \times 10^{14}$  and  $5 \times 10^{14} cm^{-2}$ . This was followed by carbon implantation with doses of  $2.34 \times 10^{14}$ ,  $9.78 \times 10^{14}$  and  $4.44 \times 10^{14} cm^{-2}$ , respectively, with corresponding energies of 25, 12.5 and 5 keV. Simulations showed that this procedure yielded a flat carbon profile. A 30 min, 450 °C anneal was used to remove end of the range damage. A 30 min anneal at 700 °C was used for the SPE growth.

High quality layers could be fabricated with carbon concentrations up to 1 atomic per cent by this technique. FTIR spectroscopy measurements showed that the carbon occupies substitutional lattice sites. Film stability was studied in the temperature range 810-925 °C and the changes in strain were measured by double crystal ray rocking curves. Carbon and oxygen concentrations were measured by SIMS and microstructure by TEM. On annealing the layers at 875 °C for 240 min, the 607  $cm^{-1}$  local mode due to substitutional carbon decreased and a broad peak at 810  $cm^{-1}$  was observed. On annealing the layers for 1200 min at the same temperature, the local mode disappeared and the broad peak became stronger indicating the precipitation of  $SiC_2$ .

### 2.3 Growth of $Ge_{1-y}C_y$ Strained Layers

Metastable  $Ge_{1-y}C_y$  alloys have been prepared by MBE under nonequilibrium conditions at relatively low growth temperatures with significant carbon concentrations<sup>49-52</sup> of  $y \approx 0.01$ . The pure germanium



layer's growth on silicon shows a typical Stranski-Krastanov (SK) mode, i.e. the growth starts in a two-dimensional mode up to a certain thickness and transition occurs to a three-dimensional island mode. The use of surfactant can inhibit three-dimensional island formation. Osten<sup>49,50</sup>, *et al.* applied the concept of antimony-mediated growth for the preparation of two-dimensionally grown  $Ge_{1-y}C_y$  layers on silicon. First a silicon buffer layer was grown followed by deposition of one monolayer of antimony. A 300 Å  $Ge_{1-y}C_y$  layer was then deposited with a growth rate of 0.125 Å s<sup>-1</sup>. The substrate temperature was 500 °C during the whole growth process. The amount of carbon co-evaporated with germanium was adjusted to attain a total carbon concentration of 1 per cent. The reflection high energy electron diffraction (RHEED) technique was used to monitor the in-plane lattice spacing of the layer during the growth. Lattice constants perpendicular to the interface ( $a_{\perp}$ ) and parallel to the interface ( $a_{\parallel}$ ) were also measured using X-ray techniques and strain in the layers was determined. Kolodzey<sup>51</sup>, *et al.* have grown crystalline germanium-carbon alloys having a cubic diamond lattice on silicon (100) using MBE at 600 °C. Measurements on thick relaxed alloy layers showed that up to 3 atomic per cent carbon was incorporated, which reduced the lattice constant and increased the energy gap (0.875 eV) compared to bulk germanium.

#### 2.4 Growth of Alloy Layers Containing Tin

One approach for realisation of a direct energy gap group IV alloy system involves alloying tin with silicon or germanium to form epitaxially stabilised diamond cubic  $Sn_xGe_{1-x}/Ge$  and  $Sn_xSi_{1-x}/Si$  heterostructures. Growth of tin-based heterostructures is challenged by the large lattice mismatch between  $\alpha$ -tin and silicon (19.5 per cent), very low solid solubility of tin in crystalline silicon ( $5 \times 10^{19} \text{ cm}^{-3}$ ), and pronounced tin segregation to the surface during growth at ordinary silicon epitaxy temperatures ( $T > 400 \text{ °C}$ ). Growth conditions similar to MBE on antimony delta-doped layers<sup>53</sup> in silicon had to be used for the growth incorporating tin at high fractions while maintaining a high epitaxial quality. Min<sup>54</sup>, *et al.* have fabricated ultra thin, coherently strained  $Sn/Si$  and  $Sn_xSi_{1-x}/Si$  alloy quantum well

structures with substitutional tin incorporation far in excess of the equilibrium solubility limit *via* substrate temperature and growth flux modulations in MBE. Tin/silicon single and multiple quantum wells with tin coverage up to 1.3 monolayer,  $Sn_{0.05}Si_{0.95}/Si$  multiple quantum wells of up to 2 nm and  $Sn_{0.16}Si_{0.84}/Si$  multiple quantum wells up to 1.1 nm were determined to be pseudomorphic.

He<sup>55</sup>, *et al.* grew strain-compensated epitaxial layer of  $Si_y(Sn_xC_{1-x})_{1-y}$  alloy films on silicon (100) with composition of tin and carbon greatly exceeding their normal equilibrium solubility in silicon. Amorphous  $SiSnC$  alloys were deposited by molecular beam deposition from solid sources followed by thermal annealing. *In situ* monitoring of crystallisation rate was done using time-resolved reflectivity. SPE for  $Si_{0.98}Sn_{0.01}C_{0.01}$  occurs at a rate about 20 times slower than that of pure silicon. The film was found to be dislocation free with good substitutionality of tin and carbon.

#### 2.5 Growth of Strained-Silicon on Relaxed Buffer Layers

The present status of growth of strained silicon on relaxed  $SiGe$  buffer layers on silicon using various techniques has been reviewed. Experimental studies for the last few years on strained  $SiGe$  materials have resulted in the understanding of strain relaxation kinetics and optimisation of graded buffer layers wrt relaxation and surface morphology<sup>56-60</sup>. These parameters are of crucial importance as they are interdependent and are affected by growth temperature, grading rate and composition.

It is now known that the problem of high threading dislocation densities in relaxed layers may be avoided using a series of low mismatched interfaces and increasing the germanium concentration in steps (step grading) or linearly with a relatively high growth temperature<sup>28,61,64</sup>. Because of gradual increase of the lattice mismatch in such a buffer, the misfit dislocation network is distributed over the range of compositional grading rather than being concentrated at the interface to the silicon substrate. The greatly improved buffer quality *via* the compositional grading lowered the threading dislocation density by three

orders of magnitude and resulted in a much improved electron mobility at low temperatures. Strained layer epitaxial growth on patterned substrates has been attempted<sup>65</sup> which can reduce epilayer threading dislocation densities by up to two orders of magnitude.

It appears that the competition between dislocation nucleation and propagation determines the final threading dislocation density in the film. The compositional grading is believed to promote propagation while suppressing nucleation of dislocations and to lead to reduced amounts of surface strain, and thus allowing higher growth temperatures<sup>66,67</sup>. In fact, the use of a compositionally graded, relaxed,  $Si_{1-x}Ge_x$  buffer layer has been advocated as virtual substrate and allows the strain in the film to be tailored at will<sup>8</sup>.

Powell<sup>68</sup>, *et al.* proposed a method for producing an almost dislocation-free relaxed  $SiGe$  buffer layer on silicon on insulator (SOI) substrates. In this process, the top silicon layer on a wafer-bonded or oxygen-implanted SOI substrate is etched back to an ultra thin layer (50 nm or less). The chemical bond at the  $Si/SiO_2$  interface is weak enough so that silicon layer can be considered as quasi-free-standing. When this is used as a substrate for the growth of a thick  $SiGe$  epitaxial film, it will be energetically favourable for the ultra thin silicon layer to relax rather than the  $SiGe$  layer itself. If this happens, the threading ends are terminated at the weakly bonded  $Si/SiO_2$  interface and the  $SiGe$  epitaxial layer relaxes without the generation of threading dislocations within the  $SiGe$  layer.

Many methods exist for deposition of strained silicon on thick relaxed  $Si_{1-x}Ge_x$  films on silicon. Gibbons<sup>69</sup>, *et al.* at Stanford were one of the first groups to demonstrate high quality relaxed thick  $Si_{1-x}Ge_x$  film on silicon. The lamp-heated limited reaction processing reactor (LRPCVD)<sup>35,69</sup> was used to grow linearly-graded  $SiGe$  buffer layers and strained silicon. High quality, epitaxial, relaxed  $Si_{1-x}Ge_x$  layers have been grown by RTCVD by Jung<sup>70</sup>, *et al.* Further improvements of the relaxed buffer (step-graded) layer formation using APCVD with intermediate *in situ* annealing at high temperature have been reported by Kissinger<sup>71</sup>, *et al.* Threading dislocation densities as low as  $100\text{ cm}^{-2}$  were found

indicating that most of the misfit dislocations really extended throughout the wafer.

High quality, completely lattice-relaxed  $SiGe$  buffer layers have been grown on silicon (100) using MBE in the range  $750\text{--}900^\circ\text{C}$  and compositional grading of the order of 10 per cent  $\text{m}^{-1}$  or less with final germanium concentrations of about 30 per cent. Xie<sup>72</sup>, *et al.* have grown compositionally graded relaxed  $Si_{1-x}Ge_x$  buffer layers on silicon with various composition gradients and temperatures. The authors reported a threading dislocation density in fully relaxed  $SiGe$  buffer layers grown using both<sup>73</sup> MBE and RTCVD in the range  $10^5\text{--}10^6\text{ cm}^{-2}$ . GSMBE has also been successfully employed<sup>74,75</sup> for the growth of high quality completely lattice-relaxed step-graded,  $SiGe$  buffer layers on silicon (100) in the range  $750\text{--}800^\circ\text{C}$ . A more abrupt compositional *transience* of the  $SiGe/Si$  interface is expected in GSMBE grown quantum wells, owing to reduced germanium segregation at the heterointerface<sup>76</sup> than in those grown by solid-source MBE, where germanium segregation has been recognised as an important issue<sup>77</sup>. A method of controlling threading dislocation density in relaxed graded buffers containing 50 to 100 per cent germanium has been developed by Currie<sup>78</sup>, *et al.* using chemical-mechanical polishing (CMP) though the release of immobile dislocations located in dislocation pile ups. The characteristic cross-hatch surface roughness and the underlying strain fields of the misfit array can overlap, blocking threading-dislocation glide leading to dislocation pile ups during the growth of thick and high germanium content buffer layers.

The growth of only a micron thick relaxed buffer layer is possible<sup>79</sup> using stepwise-graded buffer based on a combination of  $Si_{1-x}Ge_x$  and  $Si_{1-x-y}Ge_xC_y$ . The buffer concept is based on the fact that the addition of carbon to a  $SiGe$  layer not only reduces the strain, but also stabilises the layer. Due to a very strong local strain field around the individual carbon atoms, dislocation glide requires a higher energy in  $SiGeC$  than in unperturbed, strain equivalent  $SiGe$  on silicon. Using this method, a threading dislocation density below  $10^5\text{ cm}^{-2}$  was obtained for 73 per cent relaxed homogeneous  $Si_{0.7}Ge_{0.3}$  layer on top of the buffer structure. A stepped  $Si_{1-x}Ge_x$  buffer with the identical thickness

and strain profile grown at the same temperature shows a threading dislocation density above  $10^7 \text{ cm}^{-2}$ . The ternary  $\text{SiGeC}$  material therefore should be considered like a new material with its own strain degree and relaxation behaviour rather than like a  $\text{SiGe}$  film with artificially reduced strain.

Structural characterisation and film quality of strained silicon layers are usually carried out by TEM (both plan view and cross-section) for the determination of defects/dislocations within the layers and measure the thickness of the layers, and energy dispersive spectroscopy (EDS) utilising a scanning TEM for film composition. Rutherford backscattering spectroscopy (RBS) also yields similar information.

High resolution X-ray diffraction (HRXRD) is typically used to determine strain. In this technique, the lattice constant, perpendicular to the sample surface,  $a_{\perp}$  is determined. To extract germanium content and strain state of the film, it is also necessary to find the  $a_{\parallel}$ . This is achieved either by measuring the germanium content by some other method (e.g. RBS) and  $a_{\parallel}$  can be measured by grazing incidence X-ray technique. An alternative technique that measures the strain in the film directly is Raman spectroscopy. Sputter-depth profiling by SIMS is used to study the chemical composition, e.g. germanium profile. However, this method has a limiting depth resolution of about 3 nm and cannot give a reasonable profile for ultra thin films.

Fitzgerald<sup>61,80</sup> *et al.* used triple-crystal X-ray diffraction and conventional plan-view and cross-sectional TEM for the determination of strain relaxation. Compositionally graded (10 per cent germanium/ $\mu\text{m}$ )  $\text{Si}_{1-x}\text{Ge}_x$  films grown at by both MBE and RTCVD at 900°C reveal that for  $0.10 < x < 0.53$  the layers are totally relaxed.  $\text{Si}_{1-x}\text{Ge}_x$  cap layers grown on these graded layers are threading-dislocation-free when examined with plan-view and cross-sectional TEM. Electron beam induced current (EBIC) images were used to count the low threading dislocation densities. The dislocation densities measured by EBIC from MBE grown samples with final germanium concentrations of 23, 32, and 50 per cent were found to be  $4.4 \times 10^5 \pm 5 \times 10^4$ ,  $1.7 \times 10^6 \pm 1.5 \times 10^5$ , and  $3.0 \times 10^6 \pm 2 \times 10^6 \text{ cm}^{-2}$ , respectively.

## 2.6 Growth of Poly-Silicon-Germanium Films

Doped polycrystalline silicon (poly-silicon) is commonly used as gate material in MOS structures and as contact material for bipolar transistors. Poly- $\text{SiGe}$  film has emerged as a new material for advanced CMOS technology and low temperature TFT fabrication for large area display electronics. Commonly used source gases for deposition of poly- $\text{SiGe}$  are  $\text{SiH}_4$  and  $\text{GeH}_4$  in the range 400-600 °C.

RTCVD has been employed<sup>81</sup> to grow poly- $\text{SiGe}$  films. However, these films suffer from higher oxygen content and difficulty for nucleation on oxide. Very low pressure plasma CVD (VLPCVD) has been found to yield high quality films on oxidised silicon substrates at a lower temperature (400-600 °C) and pressures  $< 4$  mTorr using an RF power of 4 W only. Compared to LPCVD, the RPCVD gives higher growth rate, smaller grain sizes, direct deposition on oxide, improved structural properties, such as smoother surface and a more columnar grain structure.

King<sup>82</sup>, *et al.* also used the conventional LPCVD technique to deposit polycrystalline  $\text{Si}_{1-x}\text{Ge}_x$  films of different compositions at 625 °C and at pressures between 0.1-0.2 Torr using  $\text{SiH}_4$  and  $\text{GeH}_4$  as the precursor gas sources. The films were heavily doped with boron and phosphorus by ion implantation at a dose of  $4 \times 10^{15} \text{ cm}^{-2}$  and energy 20 keV (for boron) and 60 keV (for phosphorus) and annealed<sup>83</sup> at 900 °C for 40 min in argon. The resistivity of boron-doped films was substantially less than that of poly-silicon films with the same doping level, the resistivity decreasing with germanium mole fraction up to  $x = 0.6$ . On the other hand, the resistivity of phosphorus-doped films decreased slightly up to a germanium mole fraction of  $x = 0.45$  and increased considerably for higher germanium mole fractions. The rapid thermal annealing led to a further reduction of resistivity at a higher germanium mole fraction even at a low peak<sup>84</sup> anneal temperature (500-700 °C). It was thus evident that the temperature required to activate boron decreases dramatically with germanium content. For example, as reported<sup>83,85</sup>, the resistivity of  $\text{Si}_{1-x}\text{Ge}_x$  of thickness

25 nm annealed for 30 s at 500 °C is about 10  $\Omega$ -cm which is half of that of the silicon film annealed for 30 s at 900-1000 °C. The mobility also increases significantly with germanium content. Heavily boron-doped poly- $\text{Si}_{1-x}\text{Ge}_x$  film with  $x = 0.5$  may be a superior gate electrode material for MOSFETs and as a good interconnect layer in VLSI. On the other hand, heavily phosphorus-doped poly- $\text{Si}_{1-x}\text{Ge}_x$  films degrade with increasing germanium content above 35 per cent. Since the electron affinity does not change appreciably with the mixing of germanium in silicon, the work function of  $p$ -type  $\text{Si}_{1-x}\text{Ge}_x$  can be more effectively controlled by changing the germanium content as compared to the  $N$ -type material. This was experimentally confirmed<sup>83</sup> by King, *et al.*

Recently, Bang<sup>86</sup>, *et al.* reported sheet resistance, Hall mobility, and effective carrier concentration as a function of annealing parameters for boron and phosphorous ion implanted films of poly-silicon,  $\text{Si}_{0.75}\text{Ge}_{0.25}$ , and  $\text{Si}_{0.50}\text{Ge}_{0.50}$  films. The films were ion implanted with boron or phosphorous at dosages between  $5 \times 10^{14}$  and  $4 \times 10^{15}$   $\text{cm}^{-2}$ , and then thermally annealed between 550-650 °C for 0.25-120 min. Boron-doped films showed decreasing minimum sheet resistance with increasing germanium mole fraction (up to  $x = 0.51$ ) with extended annealing,

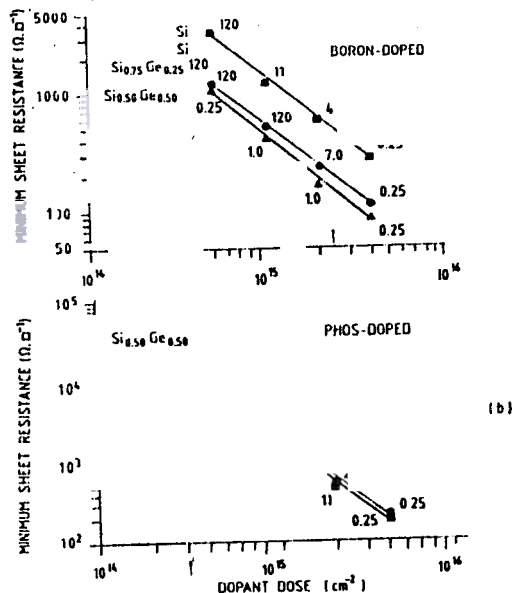


Figure 10. Minimum sheet resistance of (a) boron and (b) phosphorous-doped poly- $\text{Si}_{1-x}\text{Ge}_x$  thin films vs dopant dose. Anneal temperature is 650 °C and anneal times (in min.) required to reach minimum sheet resistances are indicated by each data point.

while phosphorous-doped films exhibited the reverse trend as discussed earlier. Figure 10 shows the minimum measured sheet resistances of boron and phosphorous-doped films versus anneal conditions, implant dose, and germanium mole fraction.

## 2.7 Growth of Hydrogenated Amorphous Silicon-Germanium Alloys

Hydrogenated amorphous silicon-germanium alloys are being developed for the narrow bandgap material in tandem solar cells, for optical detection and image sensing. The bandgap of  $a\text{-SiGe:H}$  can be varied from 1.75–1.0 eV by changing the content of germanium and make the material suitable for detection of light emitted from commercial laser diodes or LED. The thin film can be deposited at a low temperature of about (250 °C) on glass substrates.

CVD methods, such as RPECVD, microwave plasma CVD and photo CVD have been used for growing  $a\text{-SiGe:H}$  thin films. The films are deposited by mixing hydrogen with source gases:  $\text{SiH}_4$  and  $\text{GeH}_4$ . The bandgap is primarily controlled by the germane fraction  $f = \text{GeH}_4 / (\text{GeH}_4 + \text{SiH}_4)$ . Typical conditions of rf plasma-assisted deposition are: rf power 30-60 mW/ $\text{cm}^2$ , pressure 0.2 - 1.0 Torr, flow rates of  $\text{GeH}_4\text{-SiH}_4$  mixture 2-20 sccm, hydrogen flow rate of 5-50 sccm. Dilution with hydrogen causes a small decrease in the bandgap and improves the structural and electronic properties. In the presence of diluent hydrogen gas, the dissociation of  $\text{GeH}_4$  is enhanced relative to  $\text{SiH}_4$  and the incorporation of germanium is thereby increased<sup>87</sup>.

Evidence from small angle ray scattering confirms that the degradation of electronic properties of  $a\text{-SiGe:H}$  films with germanium content  $> 0.2$  is due to microstructural growth. Microstructural defects can be removed to some extent by proper use of hydrogen dilution of source gases and by controlling the rf power density.

## 3. CONCLUSION

A critical review on growth of group IV binary alloy films, in particular,  $\text{SiGe}$ ,  $\text{SiC}$ ,  $\text{GeC}$  and  $\text{SiSn}$  has been made. Various growth techniques, including MBE, CVD and SPE using implantation are compared.

MBE offers perhaps the broadest range of growth conditions and mostly used as a research tool, but MBE cannot be regarded as production-friendly. UHV/CVD offers the possibility of multiwafer growth, which is certainly attractive for volume production. APCVD, using the dichlorosilane chemistry, represents revolutionary development. It can be stated that insight into the detailed growth mechanism is rapidly progressing since a few years now, based on investigations of the fundamental surface science studies. There now exists a detailed, and mostly quantitative understanding of the epitaxial growth and cleaning procedures. However, growth rate data in the low temperature regime as a function of pressure over a broader pressure range ( $10^{-3}$  - 100 Torr) is needed. Additionally, fundamental surface studies using modern analytical techniques, preferably in real CVD conditions in view of the important role played by hydrogen, would be necessary to remove much of the uncertainty from the development of epitaxial growth processes.

Compatibility of binary alloy films with standard silicon IC technology requires that high temperature step avoided after the growth of the films. Since standard silicon processing steps, such as implantation annealing, typically exceed the strained layer deposition temperature, thermal stability of strained layers is of utmost importance. The Matthews-Blakeslee curve imposes severe limitations on stable-strained layer thickness and germanium concentration. Understanding the relaxation processes of metastable group IV alloy layers is imperative if thicknesses and germanium or other constituent concentrations greater than the equilibrium curve are needed.

## REFERENCES

- Meyerson, B.S. UHV/CVD growth of *Si* and *Si-Ge* Alloys: Chemistry, physics, and device applications. *Proceedings IEEE*, 1992, **80**, 1592-608.
- 2 Bean, J.C. Silicon-based semiconductor heterostructures: Column IV bandgap engineering. *Proceedings IEEE*, 1992, **80**, 571-87.
- Jain, S.C. Germanium-silicon strained layers and heterostructures. Academic Press Inc., New York, 1994.
- 4 Kasper, E. (Ed). Properties of strained and relaxed silicon germanium. INSPEC, Institute of Electrical Engineers, London, 1995.
- 5 Konig, U. & Daembkes, H. *SiGe* HBTs and HFETs. *Solid-State Electronics*, 1995, **38**, 1595-602.
- 6 People, R. Physics and applications of  $Ge_xSi_{1-x}/Si$  strained layer heterostructures. *IEEE J. Quantum Elec.*, 1986, **QE-22**, 1696-710.
- 7 Nayak, D.K. & Chun, S.K. Low field mobility of strained *Si* on (100)  $Si_{1-x}Ge_x$  substrate. *Appl. Phys. Lett.*, 1994, **64**, 2514-516.
- 8 Schaffler, F. High-mobility *Si* and *Ge* structures. *Semicond. Sci. Technol.*, 1997, **12**, 1515-549.
- 9 Maiti, C.K.; Bera, L.K. & Chattopadhyay, S. Strained-*Si* heterostructure field effect transistors. *Semicond. Sci. Technol.*, 1998, **13**, 1225-246.
10. Kasper, E. & Falco, C.M. Molecular beam epitaxy of silicon, silicon alloys, and metals. In *Advanced silicon and semiconducting silicon-alloy-based materials and devices*, edited by J. F. A. Nijs. Institute of Physics Publishing, Bristol, 1995. pp.103-40.
11. Caymax, M.R. & Leong, W.Y. Low thermal budget chemical vapor deposition techniques for *Si* and *SiGe*. In *Advanced silicon and semiconducting silicon-alloy-based materials and devices*, edited by J.F.A. Nijs. Institute of Physics Publishing, Bristol, 1995. pp.141-83.
12. Frank, F.C. & Van der Merwe, J.H. One-dimensional dislocations, Part II. Misfitting monolayers and oriented overgrowth. *Proc. R. Soc., A* 1949, **198**, 216-25.
- 13 Matthews, J.W. & Blakeslee, A.E. Defects in epitaxial multilayers, Part-I. Misfit dislocations. *J. Cryst. Growth*, 1974, **27**, 118-25.
14. Matthews, J.W. & Blakeslee, A.E. Defects in epitaxial multilayers, Part-II. Dislocation pile ups, threading dislocations, slip lines and cracks. *J. Cryst. Growth*, 1975, **29**, 273-80.
5. Matthews, J.W. & Blakeslee, A.E. Defects in epitaxial multilayer, Part-III. Preparation of

- almost perfect multilayers. *J. Cryst. Growth*, 1976, **32**, 265-73.
16. People, R. & Bean, J.C. Calculation of critical layer thickness versus lattice mismatch for  $Ge_xSi_{1-x}/Si$  strained layer heterostructures. *Appl. Phys. Lett.*, 1985, **47**, 322-24.
  7. Van der Merwe, J.H. Crystal interfaces, Part II. Finite overgrowths. *J. Appl. Phys.*, 1963, **34**, 123-27 (see also Erratum ibid., p. 3420 (1963)).
  18. Van der Merwe, J.H. Structure of epitaxial crystal interfaces. *Surface Science*, 1972, **31**, 198-28.
  19. Matthews, J.W. Defects associated with the accommodation of misfit between crystals. *J. Vac. Sci. Technol.*, 1975, **12**, 126-33.
  20. Bean, J.C.; Feldman, L.C.; Fiory, A. T.; Nakahara S. & Robinson, I.K.  $Ge_xSi_{1-x}/Si$  strained layer superlattice growth by molecular beam epitaxy. *J. Vac. Sci. Technol.*, A, 1984, **2**, 436-40.
  21. Kasper, E. Growth and properties of  $Si/SiGe$  superlattices. *Surface Science*, 1986, **174**, 630-39.
  22. Van de Leur, R.; Schellingerhout, A.; Tuinstra, F. & Mooij, J. Critical thickness for pseudomorphic growth of  $Si/Ge$  alloys and superlattices. *J. Appl. Phys.*, 1988, **64**, 3043-50.
  23. Chidambarrao, D.; Srinivasan, G.; Cunningham, B. & Murthy, C. Effects of Peierls barrier and epithreading dislocation orientation on the critical thickness in heteroepitaxial structures. *Appl. Phys. Lett.*, 1990, **57**, 1001-3.
  24. Lo, Y.H. New approach to grow pseudomorphic structures over the critical thickness. *Appl. Phys. Lett.*, 1991, **59**, 2311-313.
  25. Kasper, E. & Herzog, H.J. Elastic strain and misfit dislocation density in  $Si_{0.92}Ge_{0.08}$  films on silicon substrates. *Thin Solid Films*, 1999, **44**, 357-70.
  26. Bean, J.C.; Sheng, T.T.; Feldman, L.C.; Fiory, A.T. & Lynch, R.T. Pseudomorphic growth of  $Ge_xSi_{1-x}$  on silicon by molecular beam epitaxy. *Appl. Phys. Lett.*, 1984, **44**, 102-04.
  27. Meyerson, B.S. Low temperature silicon epitaxy by ultra high vacuum/chemical vapour deposition. *Appl. Phys. Lett.*, 1986, **48**, 797-99.
  28. Meyerson, B.S.; Uram, K.J. & LeGoues, F. K. Cooperative phenomena in silicon/germanium low temperature epitaxy. *Appl. Phys. Lett.*, 1988, **53**, 2555-557.
  29. Murota, J.; Nakamura, N.; Kato, M. & Mikoshiba, N. Low temperature silicon selective deposition and epitaxy on silicon using the thermal decomposition of silane under ultra clean environment. *Appl. Phys. Lett.*, 1989, **54**, 1007-9.
  30. Racanelli, M. & Greve, D. Low temperature selective epitaxy by ultrahigh vacuum chemical vapour deposition from  $SiH_4$  and  $GeH_4$ . *Appl. Phys. Lett.*, 1991, **58**, 2096-98.
  31. Greve, D.W. & Racanelli, M. Construction and operation of an ultrahigh vacuum chemical vapour deposition epitaxial reactor for growth of  $Ge_xSi_{1-x}$ . *J. Vac. Sci. Technol. B*, 1990, **8**, 511-15.
  32. Green, M.L.; Brasen, D.; Temkin, H.; Yadavish, R.D.; Boone, T.; Feldman, L.C.; Geva, M. & Spear, B.E. High gain  $Si-Ge$  heterojunction bipolar transistors grown by rapid thermal chemical vapour deposition. *Thin Solid Films*, 1990, **184**, 107-11.
  33. Green, M.L.; Weir, B.E.; Brasen, D.; Hsieh, W. F.; Higashi, G.; Feyngson, A.; Feldman, L.C. & Headrick, R.L. Mechanically and thermally stable  $Si-Ge$  films and heterojunction bipolar transistors grown by rapid thermal chemical vapor deposition at 900 °C. *J. Appl. Phys.*, 1991, **69**, 745-51.
  34. Garone, P.; Sturm, J.C.; Schartz, P.V.; Schwartz, S.A. & Wilkens, B.J. Silicon vapor phase epitaxial growth catalysis by the presence of germane. *Appl. Phys. Lett.*, 1990, **56**, 1275-277.

35. Hoyt, J.; King, C.A.; Noble, D.B.; Gronet, C.M.; Gibbons, J.F.; Scott, M.P.; Laderman, S.S.; Rosner, S.J.; Nauka, K.; Turner, J. & Kamins, T.I. Limited reaction processing: Growth of  $Si_{1-x}Ge_x/Si$  for heterojunction bipolar transistor applications. *Thin Solid Films*, 1990, **184**, 93-106.
36. Dutartre, D.; Warren, P.; Berbezier, I. & Perret, P. Low temperature silicon and  $Si_{1-x}Ge_x$  epitaxy by rapid thermal chemical vapour deposition using hydrides. *Thin Solid Films*, 1992, **222**, 52-56.
37. Sedgwick, T.O.; Berkenblit, M. & Kuan, T.S. Low temperature selective epitaxial growth of silicon at atmospheric pressure. *Appl. Phys. Lett.*, 1989, **54**, 2689-691.
38. Hsu, T.; Anthony, B.; Qian, R.; Irby, J.; Kinosky, D.; Mahajan, A.; Banerjee, S.; Magee, C. & Tasch, A. Advances in remote plasma-enhanced chemical vapour deposition for low temperature *in situ* hydrogen plasma clean and  $Si$  and  $Si_{1-x}Ge_x$  Epitaxy. *J. Electron. Mater.*, 1992, **21**, 65-74.
39. Posthill, J.B.; Rudder, R.A.; Hattangady, S.V.; Fountain, G.G. & Markunas, R.J. On the feasibility of growing dilute  $C_xSi_{1-x}$  epitaxial alloys. *Appl. Phys. Lett.*, 1990, **56**, 734-36.
40. Iyer, S.S.; Eberl, K.; Goorsky, M.S.; LeGoues, F.K. & Tsang, J.C. Synthesis of  $Si_{1-y}C_y$  alloys by molecular beam epitaxy. *Appl. Phys. Lett.*, 1992, **60**, 356-58.
41. Iyer, S.S.; Eberl, K.; Powell, A.R. & Ek, B.R.  $Si_{1-x-y}Ge_xC_y$  ternary alloys-extending  $Si$ -based heterostructures. *Microelectronic Engineering.*, 1992, **19**, 351-56.
42. Eberl, K.; Iyer, S. S.; Tsang, J. C.; Goorsky, S. S. & LeGoues, F. K. The growth and characterization of  $Si_{1-y}C_y$  alloys on  $Si(001)$  substrate. *J. Vac. Sci. Technol., B*, 1992, **10**, 934-36.
43. Goorsky, M. S.; Iyer, S. S.; Eberl, K.; LeGoues, F.; Angilelto, J. & Cardone, F. Thermal stability of  $Si_{1-x}C_x/Si$  strained layer superlattices. *Appl. Phys. Lett.*, 1992, **60**, 2758-760.
44. Eberl, K.; Iyer, S.S. & LeGoues, F.K. Strain symmetrisation effects in pseudomorphic  $Si_{1-y}C_y/Si_{1-x}Ge_x$  superlattices. *Appl. Phys. Lett.*, 1994, **64**, 739-41.
45. Faschinger, W.; Zerlauth, S.; Bauer, G. & Palmethofer, L. Electrical properties of  $Si_{1-x}C_x$  alloys and modulation-doped  $Si/Si_{1-x}Ge_x/Si$  structures. *Appl. Phys. Lett.*, 1995, **67**, 3933-935.
46. Mi, J.; Letourneau, P.; Ganiere, J.D.; Gailhanou, M.; Dutoit, M.; Dubois, C. & Dupuy, J. C. Silicon-carbon random alloy epitaxy on silicon by rapid thermal chemical vapour deposition. *Mater. Res. Soc. Symp. Proc.*, 1994, **342**, 255-59.
47. Ray, S. K.; McNeill, D. W.; Gay, D. L.; Maiti, C. K.; Armstrong, G. A.; Armstrong, B. M. & Gamble, H. S. Comparison of  $Si_{1-y}C_y$  films produced by solid-phase epitaxy and rapid thermal chemical vapor deposition. *Thin Solid Films*, 1997, **294**, 149-52.
48. Strane, J.W.; Stein, H.J.; Lee, S.R.; Picraux, S.T.; Watanabe, J.K. & Mayer, J.W. Precipitation and relaxation in strained  $Si_{1-y}C_y/Si$  heterostructures. *J. Appl. Phys.*, 1994, **76**, 3656-668.
49. Osten, H.J.; Bugiel, E. & Zaumseil, P. Antimony-mediated growth of epitaxial  $Ge_{1-y}C_y$  layers on  $Si(001)$ . *J. Cryst. Growth*, 1994, **142**, 322-26.
50. Osten H.J. & Klatt, J. *In situ* monitoring of strain relaxation during antimony-mediated growth of  $Ge$  and  $Ge_{1-y}C_y$  layers on  $Si(001)$  using reflection high energy electron diffraction. *Appl. Phys. Lett.*, 1994, **65**, 630-32.
51. Kolodzey, J.; O'Neil, P.A.; Zhang, S.; Orner, B.A.; Roe, K.; Unruh, K.M.; Swann, C.P.; White, M.M. & Shah, A.I. Growth of germanium-carbon alloys on silicon substrates by molecular beam epitaxy. *Appl. Phys. Lett.*, 1995, **67**, 1865-867.
52. Chen, ; Troger, R.T.; Roe, K.; Dashell, M. D. Jonczyk, R.; Holmes, D.S.; Wilson,

- R.J. & Kolodzey, J. Electrical properties of  $Si_{1-x}Ge_xC_y$  and  $Ge_{1-y}C_y$ . *J. Electron. Mater.*, 1997, **26**, 1371-375.
53. Zeindl, H.P.; Wegehaupt, T.; Risele, I.; Oppolzer, H.; Reissinger, H.; Tempel, G. & Koch, F. Growth and characterisation of delta-function doping layer in Si. *Appl. Phys. Lett.*, 1987, **50**, 1164-166.
  54. Min, K.S. & Atwater, H.A. Ultrathin pseudomorphic Sn/Si and  $SnSi_{1-x}/Si$  heterostructures. *Appl. Phys. Lett.*, 1998, **72**, 1884-886.
  55. He, G.; Savellano, M.D. & Atwater, H.A. Synthesis of dislocation free  $Si_y(Sn_xC_{1-x})_{1-y}$  alloys by molecular beam deposition and solid phase epitaxy. *Appl. Phys. Lett.*, 1994, **65**, 1159-161.
  56. LeGoues, F.K.; Mooney, M.M. & Chu, J.O. Crystallographic tilting resulting from nucleation limited relaxation. *Appl. Phys. Lett.*, 1993, **62**, 140-42.
  57. LeGoues, F.K.; Meyerson, B.S.; Morar, J.F. and Kirchner, P. D. Mechanism and conditions for anomalous strain relaxation in graded thin films and superlattices. *J. Appl. Phys.*, 1992, **71**, 4230-243.
  58. Mooney, P.M.; Jordan-sweet, J.L.; Ismail, K.; Chu, J. O.; Feenstra, R. M. & LeGoues, F.K. Relaxed  $Si_{0.7}Ge_{0.3}$  buffer layers for high-mobility devices. *Appl. Phys. Lett.*, 1995, **67**, 2373-375.
  59. Hsu, J.W.P.; Fitzgerald, E.A.; Xie, Y.H.; Silverman, P.J. & Cardillo, M.J. Surface morphology of relaxed  $Ge_xSi_{1-x}$  films. *Appl. Phys. Lett.*, 1992, **61**, 1293-295.
  60. Lutz, M.A.; Feenstra, R.M.; LeGoues, F.K.; Mooney, P.M. & Chu, J.O. Influence of misfit dislocations on the surface morphology of  $Si_{1-x}Ge_x$  films. *Appl. Phys. Lett.*, 1995, **66**, 724-26.
  61. Fitzgerald, E.A.; Xie, Y.-H.; Green, M.L.; Brasen, D.; Kortan, A. R.; Michel, J.; Mii, Y.-J. & Weir, B.E. Totally relaxed  $Ge_xSi_{1-x}$  layers with low threading dislocation densities grown on Si substrates. *Appl. Phys. Lett.*, 1991, **59**, 811-13.
  62. LeGoues, F.K.; Meyerson, B.S. & Morar, J.F. Anomalous strain relaxation in SiGe films and superlattices. *Physics Reviews B*, 1991, **66**, 2903-906.
  63. Schaffler, F.; Tobben, D.; Herzog, H.J.; Abstreiter, G. & Hollander, B. High-electron-mobility Si/SiGe heterostructures: Influence of the relaxed SiGe buffer layer. *Semicond. Sci. Technol.*, 1992, **7**, 260-66.
  64. Xie, Y.-H.; Fitzgerald, E. A.; Silverman, P.J.; Kortan, A.R. & Weir, B.E. Fabrication of relaxed GeSi buffer layers on Si(100) with low threading dislocation density. *Mater. Sci. Eng.*, 1992, **B14**, 332-35.
  65. Hull, R.; Bean, J.C.; Higashi, G.S.; Green, M.L.; Peticolas, L.; Bahnck, D. & Brasen, D. Improvement in heteroepitaxial film quality by a novel substrate patterning geometry. *Appl. Phys. Lett.*, 1992, **60**, 1468-470.
  66. Li, J.H.; Koppensteiner, E.; Bauer, G.; Hohnisch, M.; Herzog, H.J. & Schaffler, F. Evolution of strain relaxation in compositionally graded  $Si_{1-x}Ge_x$  films on Si(001). *Appl. Phys. Lett.*, 1995, **67**, 223-25.
  67. Mooney, P.M.; Jordan-Sweet, J.L.; Chu, J.O. & LeGoues, F.K. Evolution of strain relaxation in step-graded SiGe/Si structures. *Appl. Phys. Lett.*, 1995, **66**, 3642-644.
  68. Powell, A.R.; Iyer, S.S. & LeGoues, F.K. New approach to the growth of low dislocation relaxed SiGe material. *Appl. Phys. Lett.*, 1994, **64**, 1856-858.
  69. Gibbons, J.F.; Gronet, C.M. & Williams, K.E. Limited reaction processing: Silicon epitaxy. *Appl. Phys. Lett.*, 1985, **47**, 721-23.
  70. Jung, K.H.; Kim, Y.M. & Kwong, D.L. Relaxed  $Ge_xSi_{1-x}$  films grown by rapid thermal processing chemical vapor deposition. *Appl. Phys. Lett.*, 1990, **56**, 1775-777.



71. Kissinger, G.; Morgenstern, T.; Morgenstern, G. & Richter, H. Stepwise equilibrated graded  $Ge_xSi_{1-x}$  buffer with very low threading dislocation density on Si(001). *Appl. Phys. Lett.*, 1995, **66**, 2083-85.
72. Xie, Y.H.; Fitzgerald, E.A.; Monroe, D.; Watson, G. P. & Silverman, P. J. From Relaxed  $GeSi$  buffers to field effect transistors: Current status and future prospects. *Jap. J. Appl. Phys.*, 1994, **33**, 2372-377.
73. Fitzgerald, E.A.; Xie, Y.H.; Monroe, D.; Silverman, P.J.; Kuo, J. M. & Kortan, A. R. Relaxed  $Ge_xSi_{1-x}$  structures for III-V integration with Si and high mobility two-dimensional electron gases in Si. *J. Vac. Sci. Technol., B*, 1992, **10**, 1807-819.
74. Nayak, D.K.; Usami, N.; Sunamura, H.; Fukatsu, S. & Shiraki, Y. Band-edge photoluminescence of  $SiGe$ /strained- $Si/SiGe$  type-II quantum wells on Si(100). *Jap. J. Appl. Phys.*, 1993, **32**, 1391-393.
75. Nayak, D.K.; Usami, N.; Fukatsu, S. & Shiraki, Y. Band-edge photoluminescence of  $SiGe$ /strained- $Si/SiGe$  type-II quantum wells on Si(100). *Appl. Phys. Lett.*, 1993, **63**, 3509-511.
76. Fukatsu, S.; Yoshida, H.; Fujiwara, A.; Takahashi, Y. & Shiraki, Y. Spectral blue shift of photoluminescence in strained layer  $Si_{1-x}Ge_x/Si$  quantum well structures grown by gas source Si MBE. *Appl. Phys. Lett.*, 1992, **61**, 804-06.
77. Kato, Y.; Fukatsu, S. & Shiraki, Y. Post-growth of a Si contact layer on air - exposed  $Si_{1-x}Ge_x/Si$  single quantum well grown by gas source molecular beam epitaxy, for use in an electroluminescent device. *J. Vac. Sci. Technol., B*, 1995, **13**, 111-17.
78. Currie, M.T.; Samavedam, S.B.; Langdo, T.A.; Leitz, C. W. & Fitzgerald, E. A. Controlling threading dislocation densities in Ge on Si using graded  $SiGe$  layers and chemical-mechanical polishing. *Appl. Phys. Lett.*, 1998, **72**, 1718-720.
79. Osten, H.J. & Bugiel, E. Relaxed  $Si_{1-x}Ge_x/Si_{1-x}Ge_xC_y$  buffer structures with low threading dislocation density. *Appl. Phys. Lett.*, 1997, **70**, 2813-815.
80. Fitzgerald, E.A.; Xie, Y.H.; Brasen, D.; Green, M.L.; Michel, J.; Freeland, P.E. & Weir, B.E. Elimination of dislocations in heteroepitaxial MBE and RTCVD  $Ge_xSi_{1-x}$  grown on patterned Si substrates. *J. Electron. Mater.*, 1990, **19**, 949-55.
81. King, C.A.; Hoyt, J.L.; Gronet, C.M.; Gibbons, J.F.; Scott, M.P. & Turner, J.  $Si/Si_{1-x}Ge_x$  heterojunction bipolar transistors produced by limited reaction processing. *IEEE Electron Devices. Lett.*, 1989, **EDL-10**, 52-54.
82. King, T.J. & Saraswat, K.C. Deposition & properties of low pressure chemical-vapor deposited polycrystalline silicon-germanium films. *J. Electrochem. Soc.*, 1994, **141**, 2235-241.
83. King, T.J.; McVittie, J.P.; Saraswat, K.C. & Pfriester, J.R. Electrical properties of heavily doped polycrystalline silicon-germanium films. *IEEE Trans. Electron Devices.*, 1994, **41**, 228-32.
84. King, T.J. & Saraswat, K.C. A low temperature ( $\leq 550$  °C) silicon-germanium MOS thin-film transistor technology for large-area electronics. *In IEEE IEDM Technical Digest.*, 1991, 567-70.
85. King, T.J.; Pfriester, J.R.; Scott, D.J.; McVittie, J.P. & Saraswat, K.C. A polycrystalline  $SiGe$  gate CMOS technology. *In IEEE IEDM Technical Digest*, 1990. 253-56.
86. Bang, D.S.; Cao, M.; Wang, A.; Saraswat, K.C. & King, T.J. Resistivity of boron and phosphorous-doped polycrystalline  $Si_{1-x}Ge_x$  films. *Appl. Phys. Lett.*, 1995, **66**, 195-97.
87. Middy, A.R.; De, S.C. & Ray, S. Improvement in the properties of a- $SiGe:H$  films: Roles of deposition rate and hydrogen dilution. *J. Appl. Phys.*, 1993, **73**, 4622-630.